

A possible function of *Nik-related kinase* in the labyrinth layer of delayed delivery mouse placentas

Hiroshi YOMOGITA^{1, 2)}, Hikaru ITO^{2, 3)}, Kento HASHIMOTO²⁾, Akihiko KUDO⁴⁾, Toshiaki FUKUSHIMA⁵⁾, Tsutomu ENDO²⁾, Yoshikazu HIRATE²⁾, Yoshihiro AKIMOTO⁴⁾, Masayuki KOMADA⁵⁾, Yoshiakira KANAI⁶⁾, Naoyuki MIYASAKA¹⁾ and Masami KANAI-AZUMA²⁾

¹⁾Department of Perinatal and Women's Medicine, Tokyo Medical and Dental University, Tokyo 113-8510, Japan

²⁾Center for Experimental Animals, Tokyo Medical and Dental University, Tokyo 113-8510, Japan

³⁾Research Facility Center for Science and Technology, Kagawa University, Kagawa 761-0793, Japan

⁴⁾Department of Microscopic Anatomy, Kyorin University School of Medicine, Tokyo 181-8611, Japan

⁵⁾Cell Biology Center, Tokyo Institute of Technology, Kanagawa 226-8503, Japan

⁶⁾Department of Veterinary Anatomy, University of Tokyo, Tokyo 113-8657, Japan

Abstract. In mice and humans, *Nik-related protein kinase (NrK)* is an X-linked gene that encodes a serine/threonine kinase belonging to GCK group 4. *Nrk* knockout (*Nrk* KO) mice exhibit delayed delivery, possibly due to defective communication between the *Nrk* KO conceptus and its mother. However, the mechanism of delayed labor remains largely unknown. Here, we found that in pregnant mothers with the *Nrk* KO conceptus, the serum progesterone (P4) and placental lactogen (PL-2) concentrations in late pregnancy were higher than those in the wild type. Moreover, we demonstrated that *Nrk* is expressed in trophoblast giant cells (TGCs) and syncytiotrophoblast-2 (SynT-2) in the labyrinth layer of the mouse placenta. In the human placenta, NRK is also expressed in Syn-T in villi. Both human Syn-T and mouse TGCs of the labyrinth layer are present within fetal tissues that are in direct contact with the maternal blood. The labyrinth layer of the *Nrk* KO conceptus was gigantic, with enlarged cytoplasm and Golgi bodies in the TGCs. To investigate the function of *Nrk* in the labyrinth layer, a differentially expressed gene (DEG) analysis was performed. The DEG analysis revealed that labor-promoting factors, such as prostaglandins, were decreased, and pregnancy-maintaining factors, such as the prolactin family and P4 receptor, were increased. These findings suggest that the *Nrk* KO mice exhibit delayed delivery owing to high P4 concentrations caused by the hypersecretion of pregnancy-maintaining factors, such as PL-2, from the placenta.

Key words: Delayed delivery, *Nik-related kinase*, Progesterone, Prolactin, Trophoblast giant cells

(J. Reprod. Dev. 69: 32–40, 2023)

The human gestation period is approximately 280 days. Term birth is defined as delivery between 37 weeks and 0 days and 41 weeks and 6 days. Post-term pregnancy is defined as a pregnancy lasting longer than 42 weeks. The incidence of post-term delivery is 1–10% and is associated with an increased risk of cesarean section or NICU admission [1–3]. However, the causes of post-term birth remain unclear. Primates have similarly evolved villous placentas. In several studies, mouse pregnancy has been used as a model for human pregnancy [4]. Various delayed-delivery mouse models have been reported owing to developments in gene modifications [5].

In humans and mice, pregnancy and delivery are controlled by signals from the placenta, fetus, and mother. Among the maternal signals, progesterone (P4) has a strong influence on pregnancy and delivery in mice. P4 is secreted by the corpus luteum of the ovary and suppresses labor-induction hormones such as prostaglandins (PGs), oxytocin, and their receptors. Parturition in mice is triggered by serum P4 withdrawal owing to luteolysis 18.5 days post-coitum (dpc). Repeated P4 administration to wild-type (WT) mice after

18.5 dpc causes delayed labor [6]. The signals from the placenta belong to the prolactin (PRL) family. Two PRL family members, placental lactogen (PL)-1 and PL-2, act as luteotropic factors [7–9]. Additionally, excessive PL-2 secretion delays delivery. In *Sleo2a1* KO mice, inhibition of PGE₂ uptake in the placenta promotes PL-2 secretion and delays labor [10]. PGs are secreted by the mother, fetus, and placenta and have luteolytic functions. Intrauterine infection during pregnancy causes excessive PG secretion from the fetus and placenta, thereby resulting in premature birth [11].

Nik-related kinase (NrK) is a gene cloned by Kanai-Azuma *et al.* in 1996 [12]. *Nrk* is an X-linked gene that is common to both humans and mice and encodes a serine/threonine kinase belonging to GCK group 4 [13, 14]. *Nrk* knockout (*Nrk* KO) mice exhibit delayed delivery [15]. Placental signals might be responsible for the delayed delivery of *Nrk* KO mice, as WT dams with transplanted *Nrk* KO blastocysts exhibited delayed delivery [15]. Furthermore, a recent study has suggested that *Nrk* has undergone rapid evolution unique to eutherians and is strongly associated with placental development [16, 17]. Previous studies have reported that *Nrk* is expressed in the spongiotrophoblast layer, and *Nrk* KO placentas exhibit an overgrowth of this layer [15]. Therefore, Denda *et al.* analyzed the spongiotrophoblast layers of WT and *Nrk* KO mice using two-dimensional electrophoresis; however, no obvious differences in protein production were observed between these mice [18].

Mouse placentas are composed of three layers: the decidua, spongiotrophoblast, and labyrinth. The spongiotrophoblast layer

Received: October 31, 2022

Accepted: November 23, 2022

Advanced Epub: December 24, 2022

©2023 by the Society for Reproduction and Development

Correspondence: M Kanai-Azuma (e-mail; mkanai.arc@tmd.ac.jp)

This is an open-access article distributed under the terms of the Creative Commons Attribution Non-Commercial No Derivatives (by-nc-nd) License. (CC-BY-NC-ND 4.0: <https://creativecommons.org/licenses/by-nc-nd/4.0/>)

stores nutrients, including glycogen, and secretes hormones. The labyrinth layer exchanges gas and body waste and secretes hormones. The labyrinth layer is also one of the fetal tissues in direct contact with maternal blood, which facilitates signal exchange between the mother and fetus. The mouse labyrinth layer may be a counterpart to the human chorionic villi, as it has the same function in terms of transporting nutrients between maternal and fetal circulation. Therefore, we investigated the causes of the delayed delivery in *Nrk* KO mice, focusing on the labyrinth layer.

Materials and Methods

Mice

We used knockout mice harboring a deletion in the first *Nrk* exon. Mice were generated as previously described [15]. All animal experiments were approved by and performed in accordance with the guidelines of the Center for Experimental Animals, Tokyo Medical and Dental University (Approval numbers: A2019-159C8, A2021-146C2). PCR genotyping of mice was performed using ear biopsies.

Mature female mice were housed with males for timed mating at 1500–1700 h and separated the following morning at 0900–1200 h. A copulatory plug was observed 0.5 dpc.

Human placenta

The human placenta was sampled from a patient who underwent a cesarean section at 37 weeks owing to breech position. Before the experiment, the patient was informed of the study and consented. Our study was approved by the Medical Research Institute, Tokyo Medical and Dental University (Approval number: M2019-011).

Histology and immunohistochemistry (IHC)

Placentas were collected and fixed overnight in 4% Paraformaldehyde (PFA) at 4°C. The tissues were then processed for paraffin embedding. Sections of size 7 µm thickness were sliced, deparaffinized, and rehydrated. Antigen retrieval was performed by boiling the sections for 20 min in a citrate-based antigen-unmasking solution (Vector Laboratories, Newark, CA, USA, H-3300). Endogenous peroxidase activity was removed by incubating the sample in 0.9% H₂O₂ for 30 min at 20–25°C. Nonspecific binding was blocked with 4% normal horse serum for 1 h.

The slides were incubated with a primary antibody, rabbit anti-Nrk (Merck, Darmstadt, Germany, HPA017238, 1:1000) or rabbit anti-PL-2 (MyBioSource, CA, USA, MBS7051881, 1:100), overnight at 4°C, and incubated with donkey IgG anti-rabbit IgG (H+L)-biotin (Jackson ImmunoResearch, Cambridge, UK, 711-065-152, 1:500). For colorimetric detection, slides were developed using an Elite ABC Kit (Vector Laboratories, PK-6101) and a Peroxidase Stain DAB Kit (Nacalai Tesque, Kyoto, Japan, 25985-50), counterstained with hematoxylin.

In situ hybridization (ISH) RNA scope

ISH RNA scope was performed according to the manufacturer's instructions on RNAscope® 2.5 HD Reagent Kit- BROWN user manual (Advanced Cell Diagnostic, Newark, CA, USA; #322300). Briefly, placentas at 18.5 dpc were collected and fixed overnight in 10% neutral buffered formalin (NFB) at 20–25°C. The tissues were then processed for paraffin embedding. Sections of size 5 µm thickness were sliced, deparaffinized, and rehydrated. Endogenous peroxidase activity was removed by treating the sections with 0.3% H₂O₂ for 10 min at 20–25°C.

Antigen retrieval was performed by boiling the sections for

15 min using RNAscope® Target Retrieval Reagents (Advanced Cell Diagnostic, #322000). After the sections dried completely, RNAscope® H202 and Protease Plus Reagents (Advanced Cell Diagnostic, #322330) were added at 40°C for 30 min using the HybEZ™ Hybridization System with an EZ-Batch Slide System (Advanced Cell Diagnostic, #321461). The RNAscope Target Probe against *Nrk* was incubated with the sections in accordance with the manufacturer's instructions. DAB staining was performed, and the slides were counterstained with hematoxylin.

Immunofluorescence (IF) assay

Placentas at 18.5 dpc were collected and fixed overnight in 4% PFA at 4°C. The tissues were then processed for paraffin embedding. Sections of size 5 µm thickness were sliced, deparaffinized, and rehydrated. Antigen retrieval was performed by boiling the sections for 20 min in a citrate-based antigen-unmasking solution. Non-specific binding was blocked using 4% normal horse serum for 30 min.

The following primary antibodies were used: Rabbit anti-Nrk (Merck, HPA017238, 1:100), goat anti-endomucin (R&D Systems, MN, USA, AF4666, 1:200), goat anti-proliferin (R&D Systems, AF1623, 1:200), and goat anti-IGF1r (R&D Systems, AF305-NA, 1:200), which were incubated overnight at 4°C. The secondary antibodies used were Alexa Fluor® 488 donkey anti-rabbit IgG H&L (Jackson ImmunoResearch, 711-545-152, 1:500) and Alexa Fluor® 594 donkey anti-goat IgG H&L (Abcam, Cambridge, UK, ab150132, 1:500), which were incubated for 1 h at 20–25°C. Counterstaining and mounting were performed using VECTASHIELD® with DAPI (Vector Laboratories, H-1200).

Measurement of hormone levels

Nrk KO female mice were mated with *Nrk* KO males. Heterozygous mutant (HET: X^{*Nrk*X}) female mice were mated with *Nrk* KO males. Female WT mice were mated with male WT mice.

Blood samples were collected from the right auricle of each mouse (P4; 17.5, 19.5 dpc, PL-1,2; 17.5 dpc). These samples were maintained at 20–25°C for 30 min and centrifuged at 3,000 × rpm for 10 min at 20–25°C. The supernatant was recovered, and plasma concentrations were measured using enzyme-linked immunosorbent assay (ELISA) kits (P4: Cayman Chemical, MI, USA, 582601; PL-1: MyBioSource, CA, USA, MBS7606125; PL-2: MyBioSource, MBS7606017). Absorbance was measured using a Multiskan SkyHigh Microplate Spectrophotometer (Thermo Fisher Scientific, MA, USA, A51119500C). R ver. 4.2.0 was used for statistical analysis. The Wilcoxon signed-rank test was used only for P4 measurement at 19.5 dpc, whereas the Bonferroni multiple comparison test was used for other analyses. The Wilcoxon signed-rank test was used because the P4 level at 19.5 dpc is bimodal depending on whether luteolysis occurs or not.

Mouse placental weight measurement

Whole placentas were harvested and weighed at 18.5 dpc. Labyrinth layer samples were dissected from the whole placenta. The weight ratios were divided by the weight of the dam to exclude the effect of the dam size. Student's *t*-test was performed using R ver. 4.2.0.

The cytoplasmic to nuclear (C/N) ratio measurement

Placentas were harvested at 18.5 dpc, and IF assay was performed. Goat anti-proliferin (R&D Systems, AF1623, 1:200) was used as the primary antibody. DAPI was used for nuclear staining. The number of pixels in the whole cell and nucleus were counted using ImageJ. For statistical analysis, Student's *t*-test was performed using R ver. 4.2.0.

Transmission electron microscopy (TEM)

The labyrinth layer samples were fixed in 2.5% glutaraldehyde dissolved in 0.1 M phosphate buffer (pH 7.4) for 24 h at 4°C. Following a PBS wash, the samples were fixed with 1% osmium tetroxide dissolved in 0.1 M phosphate buffer (pH 7.3) for 30 min and dehydrated using a graded series of ethanol concentrations. After the tissues were passed through propylene oxide, they were embedded in Epon 812. Ultrathin sections were cut, stained with uranyl acetate and lead citrate, and observed using TEM (IOCB, Praha, Czechia, JEM-1011; JEOL).

To measure the area occupied by the Golgi apparatus in the cytoplasm, whole-cell images of the trophoblast giant cells (TGCs) were taken at low magnification. Twenty TGC images were randomly chosen from each placental sample of three WT and three *Nrk* KO fetuses. The total Golgi area per cell section was quantified using iTEM image analysis software (Olympus Soft Imaging Solutions GmbH, Münster, Germany), in which the outline of Golgi stacks and related vesicles was traced manually using a pen tablet device. Student's *t*-test was performed using R ver. 4.2.0.

RNA extraction

Labyrinth layer samples were dissected from the entire placenta. Total RNA was extracted using a PureLink RNA Mini Kit (Thermo Fisher Scientific, 12183018A) following the manufacturer's protocol. RNA quantity and quality were assessed using NanoDrop One[®] (Thermo Fisher Scientific, 840-329700).

Bulk RNA sequencing (RNA-Seq)

Sequencing libraries were generated using the TruSeq stranded mRNA LT Sample Prep Kit for Illumina (Illumina, CA, USA) following TruSeq Stranded mRNA Reference Guide Document #1000000040498 v00. Libraries were sequenced using NovaSeq 6000 (Illumina, 20012850). Trimmed reads were mapped to the reference genome using HISAT2, a splice-aware aligner. The read count values of the known genes obtained using the *-e* option of StringTie were used as the original raw data. During data preprocessing, low-quality transcripts were filtered. Subsequently, TMM normalization was performed. Statistical analysis was performed using fold change and exactTest using edgeR for each comparison pair. Significant results were selected based on the conditions of \log_2 fold change > 1 and exact test raw *p*-value < 0.05. Volcano plots and heat maps were drawn using the 'Python' software.

Enriched gene ontology (GO) annotation and enrichment analysis

Genes with a significant difference in mRNA expression levels between the WT and *Nrk* KO mice were used to analyze GO annotation enrichment. The Database for Annotation, Visualization, and Integrated Discovery (Metascape; <http://metascape.org>) was used to test the enrichment of functional categories annotated by GO terms.

Results

Nrk is expressed in TGCs and syncytiotrophoblast-T2 of the labyrinth layer in mice

ISH and IHC were performed to detect *Nrk* expression in the mouse placenta. A previous study reported that *Nrk* was expressed in the spongiotrophoblast layer [15]. ISH results showed that *Nrk* mRNA was present not only in the spongiotrophoblast layer but also in the labyrinth layer at 18.5 dpc (Fig. 1A). The IHC analysis showed similar results at the same stage (Fig. 1B). Labyrinth-layer

cells include TGCs, syncytiotrophoblast-1 and -2 (Syn-T1 and -T2), and endothelial cells (EC). The cell types in the labyrinth layer that expressed NRK were detected using IF. NRK is expressed surrounding proliferin, which is a TGC cytoplasmic marker (Fig. 1C upper panels with white arrowheads). *Nrk* exists just below the plasma membrane of TGCs. As the TGC is present within a sinusoidal blood space, we assume that it is a sinusoidal TGC [19]. IGR1r and NRK staining patterns clearly show the cytoplasm of Syn-T2 cells (Fig. 1C, middle panels with white arrowheads). NRK did not co-localize with the EC marker endomucin (Fig. 1C, lower panels with white arrowheads).

NRK is expressed in syncytiotrophoblast in humans

To assess NRK expression in humans, the placenta of a patient who underwent cesarean section at 37 weeks of gestation owing to breech position was analyzed. The human placenta is composed of the maternal basal decidua and fetal chorionic villi. Villi are composed of Syn-T, cytotrophoblasts, mesoderm, and fetal blood vessels. Syn-T plays a central role in nutrient-waste exchange and secretes hormones, such as hCG. In the human placenta at 37 weeks, both ISH and IHC revealed that NRK was expressed in the Syn-T cells (Fig. 1D, E). Furthermore, both human Syn-T and mouse TGCs in the labyrinth layer were in direct contact with the maternal blood.

Nrk KO mice show a higher frequency of delayed delivery

The labor phenotypes were recorded for the *Nrk* KO, HET, and WT mice. In the WT intercross (WT females and WT males), the frequency of delayed delivery was only 18.1% (4/22 cases) (Table 1). In the *Nrk* KO intercross (*Nrk* KO females and *Nrk* KO males), 79.3% did not deliver within 19 dpc (23/29 cases) (Table 1). Thus, the frequency of delayed delivery was significantly higher in the *Nrk* KO intercross than in the WT intercross (Student's *t*-test, $P = 0.000057$; Table 1). When HET females were mated with *Nrk* KO males, 65.4% did not deliver within 19 dpc (53/81 cases) (Table 1). Additionally, HET mice were more prone to delayed delivery than WT mice (Student's *t*-test, $P = 0.00026$; Table 1). In late pregnancy, no difference was observed in the number of fetuses born through cesarean section between the WT, HET, and *Nrk* KO mice (one-way ANOVA, $P = 0.21$; Supplementary Fig. 1).

Nrk KO mice show increased P4 blood levels

To determine the cause of delayed delivery, we compared the levels of P4 in maternal blood in *Nrk* KO, HET, and WT mice using ELISA. At 17.5 dpc, the average P4 level of WT mice was 37,981 pg/ml, that of *Nrk* KO mice was 52,459 pg/ml, and that of HET was 38,238 pg/ml, with no significant difference (Bonferroni multiple comparison test, $P = 1.00$; Fig. 2A). However, at 19.5 dpc, the average P4 level of WT mice was 1,711 pg/ml, that of *Nrk* KO mice was 12,081 pg/ml, and that of HET mice was 11,924 pg/ml. The P4 concentration was significantly higher in the *Nrk* KO mice than in the WT mice at 19.5 dpc (Wilcoxon signed-rank test, $P = 0.0080$; Fig. 2A). Similarly, P4 levels were higher in the HET mice than in the WT mice (Wilcoxon signed-rank test, $P = 0.0073$; Fig. 2A).

In the PRL family, the average PL-1 concentration at 17.5 dpc did not differ between WT, HET, and *Nrk* KO mice (Bonferroni multiple comparison test, $P = 0.18$; Fig. 2B). In contrast, the average PL-2 concentration was higher in the *Nrk* KO mice than in the WT mice (Bonferroni multiple comparison test, $P = 0.0018$; Fig. 2C). Similarly, PL-2 levels were higher in the HET mice than in the WT mice (Bonferroni multiple comparison test, $P = 0.0046$; Fig. 2C). Further analysis of *Nrk* KO and HET mice suggested that the higher the number of *Nrk* KO placentas in the uterus, the higher the PL-2

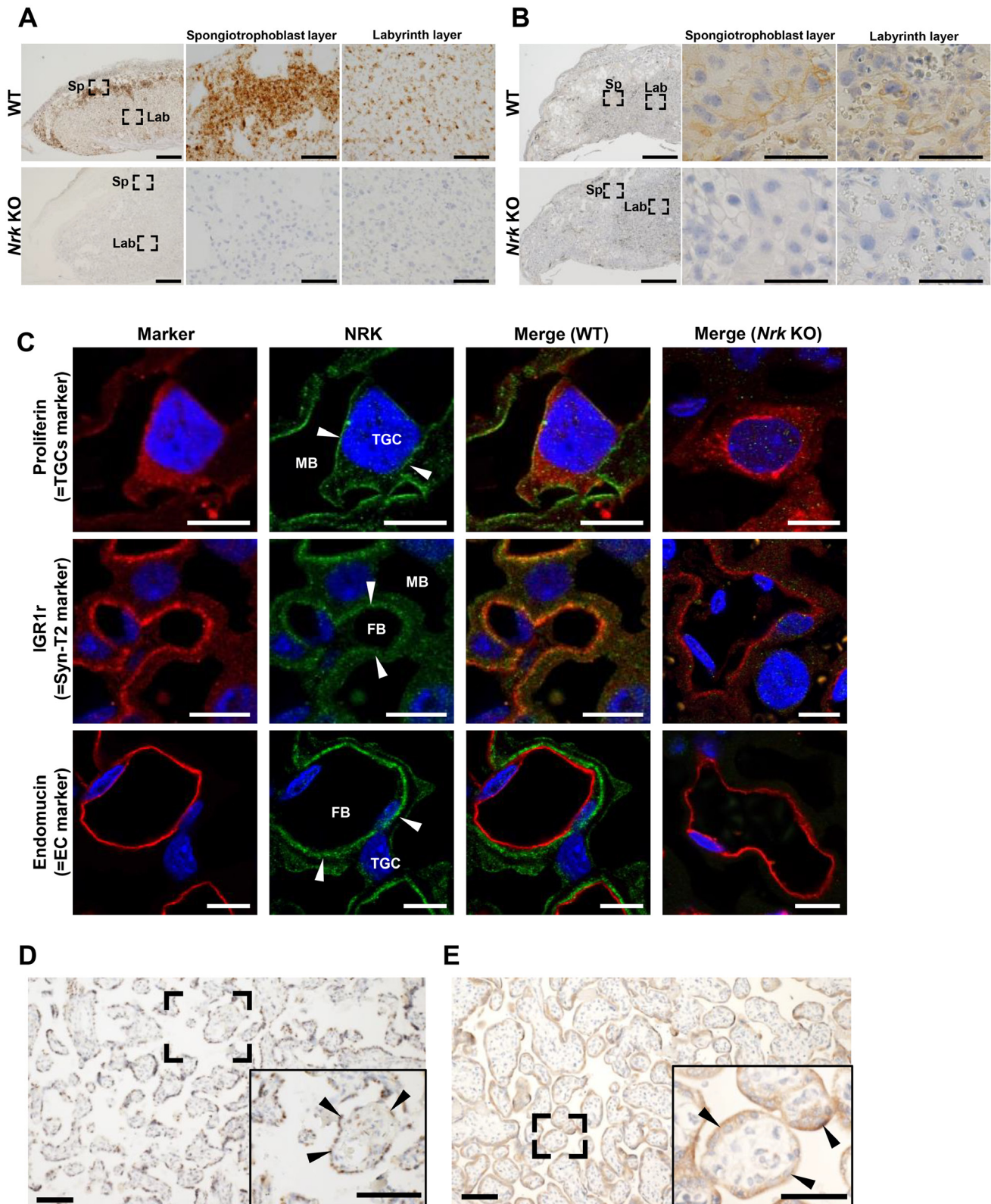


Fig. 1. *Nrk* expression site in mouse and human placenta. (A) ISH of 18.5 dpc WT mouse placentas showed dense *Nrk* staining throughout the labyrinth and spongiotrophoblast layer (scale bars: 500 μ m for left panels, 100 μ m for middle and right panels). Sp; spongiotrophoblast layer, Lab; labyrinth layer. (B) In IHC of 18.5 dpc WT mouse placentas, both the spongiotrophoblast and labyrinth layer at 18.5 dpc were stained for NRK (scale bars: 500 μ m for left panels, 50 μ m for middle and right panels). (C) IF of 18.5 dpc WT mouse placentas (scale bars: 10 μ m). Upper panels: Proliferin is a cytoplasmic marker for TGCs. NRK is expressed just below the plasma membrane of TGCs. Middle panels: IGR1r and NRK staining patterns show SynT-2. Lower panels: NRK did not colocalize with the EC marker endomucin. MB; maternal blood, FB; fetal blood. (D) ISH of the human placenta sampling due to cesarean section at 37 weeks showed dense staining of NRK in Syn-T (scale bars: 100 μ m). (E) IHC of the human placenta showed dense staining of NRK in Syn-T (scale bars: 100 μ m).

Table 1. Labor phenotype in WT, HET, and *Nrk* KO female mice

	♀ WT ♂ WT	♀ HET ♂ <i>Nrk</i> KO	♀ <i>Nrk</i> KO ♂ <i>Nrk</i> KO
Delayed delivery (After 20.5 dpc)	4 (18.1%)	53 (65.4%)	23 (79.3%)
Normal and preterm delivery (Before 19.5 dpc)	18 (81.8%)	28 (34.6%)	6 (20.6%)

In the *Nrk* KO intercross, the frequency of delayed delivery was significantly higher than in the WT intercross (Student's *t*-test, $P = 0.000057$). HET mice delivered later than WT mice when HET females were mated with *Nrk* KO males (Student's *t*-test, $P = 0.00026$). $N =$ WT 22, HET 81, *Nrk* KO 29 mice.

concentration (Pearson's product-moment correlation, $r = 0.984$, $P = 0.00035$; Supplementary Fig. 2). IHC was performed to confirm the localization of PL-2 at 18.5 dpc. The results showed that PL-2 was expressed both in the spongiotrophoblasts and the labyrinth layer, and *Nrk* KO mice tended to show higher PL-2 expression than WT mice (Supplementary Fig. 3).

The labyrinth layer weight ratio is higher in *Nrk* KO mice

To investigate the function of *Nrk* in the labyrinth layer, we analyzed the morphology of *Nrk* KO placentas. HE staining of the placenta at 18.5 dpc revealed that the labyrinth layer in *Nrk* KO placentas was larger than that in WT placentas (Fig. 3A). We compared the placental weights between the WT and *Nrk* KO mice. The weight ratio was calculated by dividing the weight of the placenta by the weight of the dam to exclude the effect of dam size. The average ratio of the weight of the whole placenta was 3.49 for WT mice and 7.08 for *Nrk* KO mice (Fig. 3B, left; raw weight data Supplementary

Fig. 4A). Therefore, the placentas of *Nrk* KO mice were significantly heavier than those of WT mice (Student's *t*-test, $P = 1.372e-07$; Fig. 3B, left). This result is consistent with those of previous studies [15].

Furthermore, when comparing only the labyrinth layer, the weight ratio was 2.04 and 3.84 for WT and *Nrk* KO mice, respectively (Fig. 3B right; raw weight data Supplementary Fig. 4B). The labyrinth layer of *Nrk* KO mice had a significantly higher weight ratio than WT mice (Student's *t*-test, $P = 1.780e-07$; Fig. 3B, right).

Labyrinth layer TGCs have higher C/N ratio in *Nrk* KO mice

HE staining of the *Nrk* KO labyrinth layer revealed that the cytoplasm of TGCs was expanded (Fig. 3C, arrowheads). As TGCs express *Nrk* and secrete members of the PRL family, we focused on TGCs in the labyrinth layer. The C/N ratios of *Nrk* KO and WT mice TGCs were quantified (Fig. 3D), and the average C/N ratio of WT was 0.855, while that of *Nrk* KO was 1.099 (Fig. 3E). The C/N ratio of TGCs in *Nrk* KO mice was significantly higher than that in WT mice (Student's *t*-test, $P = 0.001186$; Fig. 3E). Although nuclear size was not significantly different between the WT and *Nrk* KO mice (Student's *t*-test, $P = 0.7958$; Supplementary Fig. 5A), the cytoplasm of *Nrk* KO mice was significantly larger than that of WT mice (Student's *t*-test, $P = 0.001905$; Supplementary Fig. 5B).

Golgi bodies of TGCs expand in *Nrk* KO mice

To investigate the causes of the swollen TGCs, we performed electron microscopic analysis. TEM revealed that the Golgi bodies of TGCs in *Nrk* KO mice were enlarged (Fig. 3F). The area of Golgi bodies in *Nrk* KO TGCs was 8.62 nm² and that in WT TGCs was 6.15 nm² (Fig. 3G). Golgi bodies in *Nrk* KO TGCs were significantly larger than those in WT TGCs (Student's *t*-test, $P = 0.001304$; Fig. 3G). In Syn-T2 of *Nrk* KO, the cytoplasm was strongly degenerated,

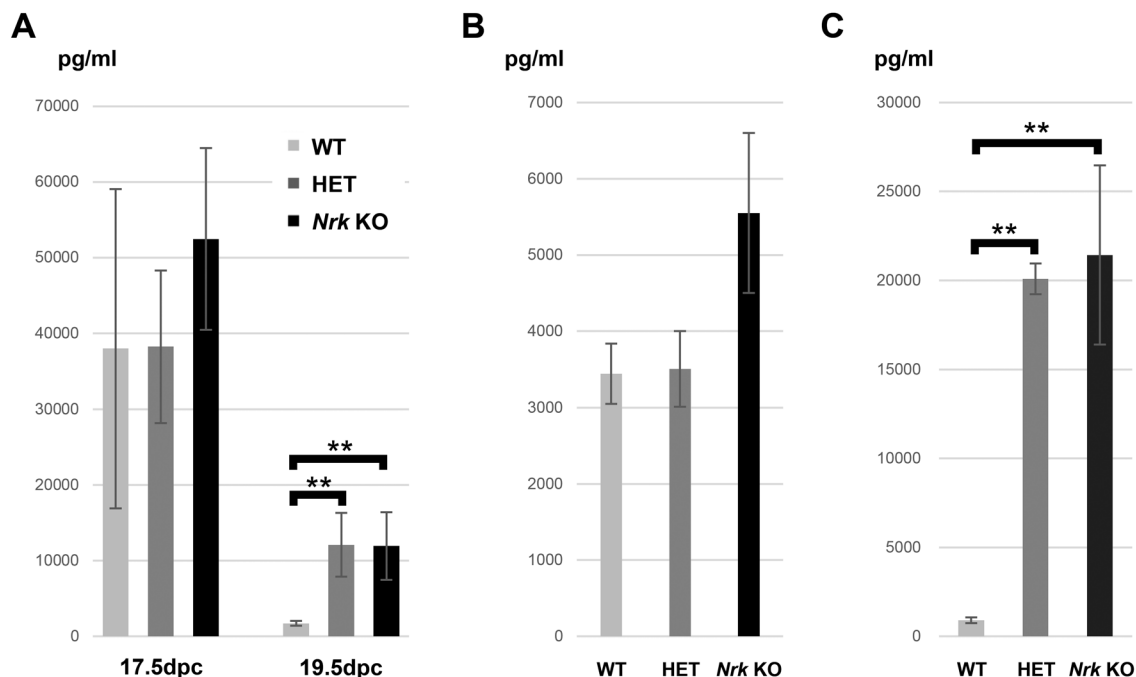


Fig. 2. Maternal blood levels of P4, PL-1, and PL-2 in late pregnancy by ELISA. (A) Maternal blood levels of P4 were measured at 17.5 dpc and 19.5 dpc. Each concentration was compared between WT, HET, and *Nrk* KO mice. $N =$ WT 10, HET 10, *Nrk* KO 16 mice; ** $P < 0.01$, Wilcoxon signed-rank test. (B) Maternal PL-1 blood levels at 17.5 dpc were compared between WT, HET, and *Nrk* KO mice. $N =$ WT 5, HET 4, *Nrk* KO 5 mice; $P = 0.18$, Bonferroni multiple comparison test. (C) Maternal PL-2 blood levels at 17.5 dpc were compared between WT, HET, and *Nrk* KO mice. $N =$ WT 5, HET 4, *Nrk* KO 5 mice; ** $P < 0.01$, Bonferroni multiple comparison test.

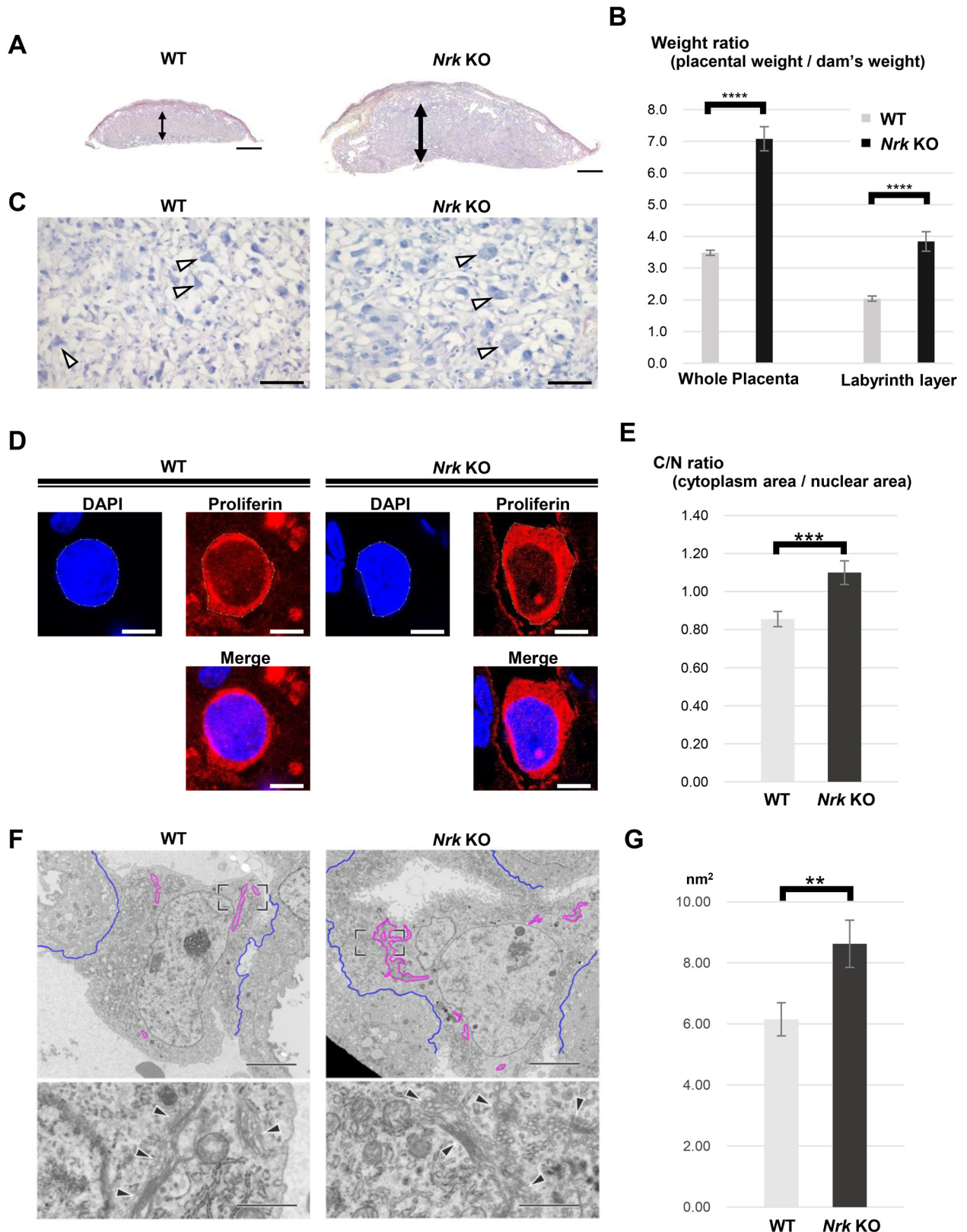


Fig. 3. The phenotype in the labyrinth layer of *Nrk* KO mice. (A) HE staining of the placenta at 18.5 dpc revealed that the *Nrk* KO labyrinth layer was larger than WT labyrinth layer (scale bars: 1000 μ m). The double arrows indicate the labyrinth layer's height. (B) The weights of the whole placenta and labyrinth layer were compared between WT and *Nrk* KO mice. $N =$ WT 28, *Nrk* KO 24 placentas; **** $P < 0.0001$, Student's t -test. (C) HE staining of WT and *Nrk* KO mice in the labyrinth layer (scale bars: 50 μ m). The open arrow heads indicate TGCs. (D) Representative images of cytoplasm and nuclear measurements (scale bars: 10 μ m). Blue; DAPI (nuclear maker), Red; Proliferin (cytoplasmic maker). (E) The C/N ratios of TGCs were compared between the WT and *Nrk* KO labyrinth layer. $N =$ WT 101, *Nrk* KO 103 cells; *** $P < 0.001$, Student's t -test. (F) TEM revealed that the Golgi bodies of TGCs in *Nrk* KO were enlarged (scale bars: 5 μ m for upper panels, 1 μ m for lower panels). The open arrow heads indicate Golgi bodies. Blue line; the border between cells, Magenta line; the Golgi area. (G) The Golgi body area of TGCs in *Nrk* KO mice was significantly larger than that in WT mice. $N =$ WT 60, *Nrk* KO 58 cells; ** $P < 0.01$, Student's t -test.

and the vacuoles were prominent (Supplementary Fig. 6).

Pregnancy-related genes are affected in NrK KO mice.

To confirm the cause of the delayed delivery, we identified DEGs between *Nrk* KO and WT mice using RNA-Seq. The labyrinth layer was bluntly peeled off at 18.5 dpc and analyzed via RNA-Seq. A total of 18,261 genes were used for the statistical analysis. In the *Nrk* KO placenta, 158 genes were upregulated and 100 genes were downregulated ($P < 0.05$, fold-change > 2 ; Fig. 4A). The GO terms included “Female pregnancy,” “Glycolipid catabolic process,” and “Hydrolysis of LPC” (Fig. 4B). From this analysis, we identified 15 genes related to pregnancy and delivery (Fig. 4C). *Progesterin and adipo Q receptor family member 9 (Paqr9)* that encodes P4 receptor was upregulated. Five PRL family members, *Prl4a1*, *Prl7a2*, *Prl7b1*, and *Prl7c1* were also upregulated (Fig. 4C). In contrast, the *PL-2* mRNA levels did not change significantly (fold change: 1.15). The expression of the labor-inducing gene *prostaglandin synthase cyclooxygenase 2 (Cox2)* was decreased (Fig. 4C). The expression of many steroid metabolism-related genes, such as *cytochrome P450 family 4 subfamily B member (Cyp4b1)*; *hydroxysteroid 11-beta dehydrogenase 2 (Hsd11b2)*; *hydroxysteroid 17-beta dehydrogenase 7 (Hsd17b7)*; *steroid 5 alpha-reductase 1 (Srd5a1)*; and *phospholipase A2 group IV (Pla2g4)*, was also altered (Fig. 4C).

Discussion

We found that *Nrk* was expressed in the labyrinth layer of mouse placenta (Figs. 1A, B). IHC revealed that *Nrk* was expressed in TGCs and Syn-T2 of the mouse labyrinth layer (Fig. 1C). NRK exists just below the plasma membrane of TGCs. This cell localization is consistent with a previous study showing that mouse NRK is localized to the plasma membrane via the citron homology domain [16]. In the human placenta, NRK was also expressed in the Syn-T of the villi (Figs. 1D, E). Both human Syn-T and mouse TGCs have the common function of exchanging substances between the mother and fetus [20]. Both cells are part of the fetal tissue that is in direct contact with maternal blood, which might facilitate the exchange of fetal signals with the mother.

Most *Nrk* KO and HET mice did not deliver before 19 dpc, with a total of 79.3% of *Nrk* KO mice exhibiting delayed delivery (Table 1). According to previous reports, some fetuses experience a prolonged gestational period depending on the mouse strain [21, 22]. In late pregnancy, there was no difference in the number of fetuses born through cesarean section between the WT, HET, and *Nrk* KO mice (one-way ANOVA, $P = 0.21$; Supplementary Fig. 1). In this study, we analyzed only WT-WT, HET-*Nrk* KO, and *Nrk* KO-*Nrk* KO crosses because the other combinations are more difficult to analyze owing to X chromosome inactivation. In the future, it will be necessary to examine detailed differences in the delivery outcomes of these other combinations as well.

At 19.5 dpc, P4 concentration in the *Nrk* KO mice was significantly higher than that in the WT mice (Fig. 2A). In a previous study, the blood P4 levels were not significantly different [15]. Because a significant difference was observed in our study, we assume that this result is due to differences in sample sizes and measurement methods. At 17.5 dpc, PL-2 concentration in the *Nrk* KO mice was higher than that in the WT mice (Fig. 2C). PL-2 concentration correlated with the number of *Nrk* KO placentas (Supplementary Fig. 2). These results imply that the cause of delayed delivery in *Nrk* KO mice may be excessive P4 secretion owing to the failure of luteolysis, which is caused by increased PL-2 production from the *Nrk* KO placenta.

Sleo2a1 KO mice also exhibit delayed labor for reasons similar to those of *Nrk* KO mice [10]. *Sleo2a1* KO mice are deficient for an organic anion transporting polypeptide 2A1, which is known as the PG transporter. This deficiency leads to a high concentration of extracellular PGE₂, thereby resulting in excessive PL-2 secretion [10]. Further studies are needed to confirm the direct molecular pathway by which P4 causes delayed parturition in *Nrk* KO mice.

Overgrowth of the spongiotrophoblast layer in *Nrk* KO mice is presumed to be due to the enhancement of the AKT pathway [16, 23]. NRK is localized inside the cell membrane and inhibits casein kinase 2, a negative regulator of phosphatase and tensin homolog (PTEN) [16]. NRK might indirectly activate PTEN through this mechanism, thereby suppressing the AKT pathway and cell hyperproliferation [16, 23]. The labyrinth layer weight of the *Nrk* KO mice was higher than that of the WT mice (Fig. 3B, Supplementary Fig. 4). Additionally, the cytoplasm of TGCs in *Nrk* KO mice was larger than that of TGCs in WT mice (Fig. 3E). These results are consistent with the TEM observations, which revealed that the Golgi apparatus, located at the midpoint of membrane trafficking, was enlarged in *Nrk* KO mice (Figs. 3F, G). We conclude that this is one of the reasons for cytoplasmic expansion in *Nrk* KO TGCs. Although the smooth endoplasmic reticulum (sER) of *Nrk* KO TGCs in the labyrinth tended to be dilated in the TEM analysis, no significant difference was observed in our measurements. As sER synthesizes steroids, this may reflect the changes in *Nrk* KO steroid-metabolizing enzymes in the DEGs (Fig. 4C). The cytoplasm of *Nrk* KO Syn-T2 cells, which also expresses *Nrk*, was strongly degenerated, and the vacuoles were prominent (Supplementary Fig. 6).

In the GO terms of the WT and *Nrk* KO labyrinth layers, pregnancy-related gene expression was significantly altered (Fig. 4B). The differential gene expression analysis revealed that the expression of some labor-related genes was altered (Fig. 4C). *Paqr9*, a P4 receptor gene, was upregulated. *Prl4a1*, *Prl7a2*, *Prl7b1*, and *Prl7c1* were upregulated, whereas *PL-1* and *PL-2* levels did not change significantly (Fig. 4C). As many types of *Prl7* were enhanced, they may be strongly related to the function of *Nrk*. However, the function of *Prl7* remains unclear. Because the molecular structures of PL-1,2 and other members of the PRL family are similar, *Prl4a1*, *Prl7a2*, *Prl7b1*, and *Prl7c1* may have luteotropic effects. PL-2 is secreted from both spongiotrophoblasts and TGCs of the labyrinth layer [24]. The IHC results for *Nrk* KO placentas showed that PL-2 was strongly expressed in both the spongiotrophoblast and labyrinth layers (Supplementary Fig. 3). DEG analysis of the labyrinth layer revealed no significant difference in *PL-2* gene expression between WT and *Nrk* KO mice. The reason for the minor increase in *PL-2* RNA despite the high concentration of PL-2 in maternal blood is unclear; therefore, whether this difference is caused by protein synthesis and/or degeneration in late pregnancy should be investigated in the future. Further studies are necessary to identify which cells in the two layers secrete PL-2 and determine its molecular function.

Cox2, a downregulated gene, is a rate-determining enzyme in PGs. In late pregnancy, PGF_{2α} regresses the corpora [25, 26]. It is unclear whether the decrease in *Cox2* is the cause or a result of delayed labor in *Nrk* KO mice. The expression of many steroid metabolism-related genes was also altered. Steroid metabolism is complex, induces labor, and maintains pregnancy. As the results of DEGs suggested abnormal steroid metabolism (Fig. 4C), it was suggested that these changes in steroid metabolism may influence gestational length [27–29].

In humans, NRK is expressed in Syn-T, which is located on the outermost side of villi (Fig. 1D, E). Similar to mice, this is the fetal

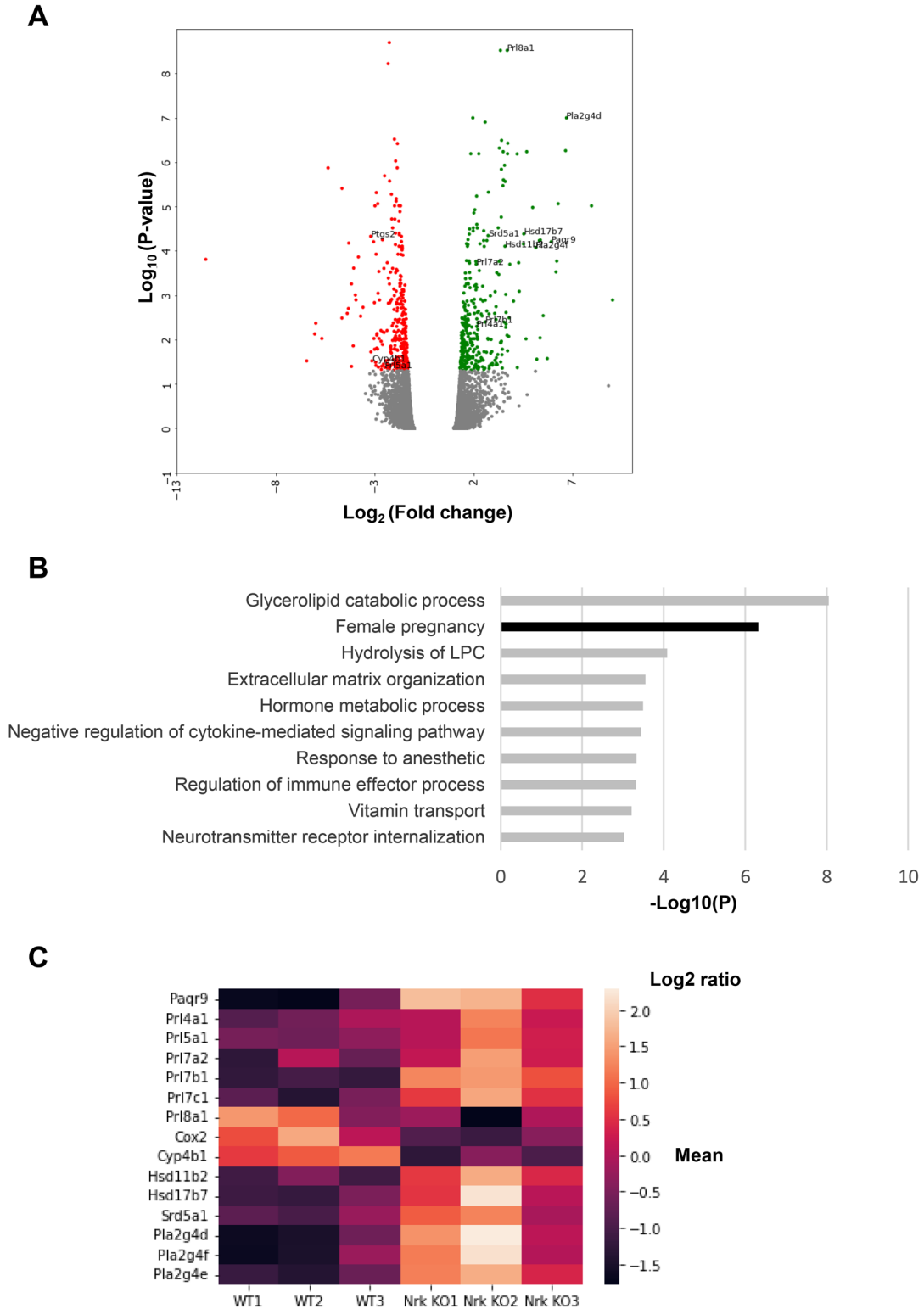


Fig. 4. DEGs: WT vs. *Nrk* KO of labyrinth layer. (A) Volcano plot of individual gene expression levels with fold change (x-axis) against P-value (y-axis) in WT and *Nrk* KO. DEGs (\log_2 fold change ≥ 1 , $P < 0.01$) are in green. DEGs (\log_2 fold change ≥ -1 , $P < 0.01$) are in red. *Nrk* (fold change -433 , P-value 0) was not plotted. (B) The top 10 GO terms. (C) Heat map of expression levels of pregnancy and delivery-related genes.

tissue in contact with maternal blood and is a convenient location for fetal-maternal signaling. On the other hand, humans have only one type of PRL [24], and because the corpus luteum disappears around 12 weeks of gestation, P4 does not change in late pregnancy [30]. In this study, we demonstrated that NRK is also expressed in the Syn-T

of human placental villi. Human NRK may have a significant impact on placentation in evolutionary biology, similar to mouse NRK. Further studies on NRK expression in the placenta during preterm labor, term labor, preterm delivery, and other conditions associated with preterm labor are needed to elucidate its function in humans.

Conflict of interests: The authors declare no conflict of interest associated with this manuscript.

Acknowledgments

The authors thank the Center for Experimental Animals, Tokyo Medical and Dental University for supporting our research, especially Kana Hayakawa, Chieko Ostuka, and Hitomi Takahashi. The authors also thank Sachie Matsubara, Junri Hayakawa, Laboratory for Electron Microscopy, and Kyorin University School of Medicine for the TEM analysis. We are grateful to Dr. Fumitoshi Ishino and Mrs. Kendall for reviewing this manuscript. This study was supported by JSPS KAKENHI (grant numbers 21H02387 and 18H02361).

References

- Vayssière C, Haumonté JB, Chanry A, Coatleven F, Debord MP, Gomez C, Le Ray C, Lopez E, Salomon LJ, Senat MV, Sentilhes L, Serry A, Winer N, Grandjean H, Verspyck E, Subtil D. French College of Gynecologists and Obstetricians (CNGOF). Prolonged and post-term pregnancies: guidelines for clinical practice from the French College of Gynecologists and Obstetricians (CNGOF). *Eur J Obstet Gynecol Reprod Biol* 2013; **169**: 10–16. [Medline] [CrossRef]
- Martin JA, Hamilton BE, Osterman MJ, Curtin SC, Matthews TJ. Births: final data for 2012. *Natl Vital Stat Rep* 2013; **62**: 1–68. [Medline]
- Linder N, Hirsch L, Fridman E, Klinger G, Lubin D, Kouadio F, Melamed N. Post-term pregnancy is an independent risk factor for neonatal morbidity even in low-risk singleton pregnancies. *Arch Dis Child Fetal Neonatal Ed* 2017; **102**: F286–F290. [Medline] [CrossRef]
- Ratajczak CK, Muglia LJ. Insights into parturition biology from genetically altered mice. *Pediatr Res* 2008; **64**: 581–589. [Medline] [CrossRef]
- Yomogita H, Miyasaka N, Kanai-Azuma M. A review of delayed delivery models and the analysis method in mice. *J Dev Biol* 2022; **10**: 10. [Medline] [CrossRef]
- Herington JL, O'Brien C, Robuck MF, Lei W, Brown N, Slaughter JC, Paria BC, Mahadevan-Jansen A, Reese J. Prostaglandin-endoperoxide synthase 1 mediates the timing of parturition in mice despite unhindered uterine contractility. *Endocrinology* 2018; **159**: 490–505. [Medline] [CrossRef]
- Galosy SS, Talamantes F. Luteotropic actions of placental lactogens at midpregnancy in the mouse. *Endocrinology* 1995; **136**: 3993–4003. [Medline] [CrossRef]
- Thordarson G, Galosy S, Gudmundsson GO, Newcomer B, Sridaran R, Talamantes F. Interaction of mouse placental lactogens and androgens in regulating progesterone release in cultured mouse luteal cells. *Endocrinology* 1997; **138**: 3236–3241. [Medline] [CrossRef]
- Zhong L, Parmer TG, Robertson MC, Gibori G. Prolactin-mediated inhibition of 20alpha-hydroxysteroid dehydrogenase gene expression and the tyrosine kinase system. *Biochem Biophys Res Commun* 1997; **235**: 587–592. [Medline] [CrossRef]
- Inagaki M, Nishimura T, Nakanishi T, Shimada H, Noguchi S, Akanuma SI, Tachikawa M, Hosoya KI, Tamai I, Nakashima E, Tomi M. Contribution of prostaglandin transporter OATP2A1/SLCO2A1 to placenta-to-maternal hormone signaling and labor induction. *iScience* 2020; **23**: 101098. [Medline] [CrossRef]
- Agrawal V, Hirsch E. Intrauterine infection and preterm labor. *Semin Fetal Neonatal Med* 2012; **17**: 12–19. [Medline] [CrossRef]
- Kanai-Azuma M, Kanai Y, Okamoto M, Hayashi Y, Yonekawa H, Yazaki K. NrK: a murine X-linked NIK (Nek-interacting kinase)-related kinase gene expressed in skeletal muscle. *Mech Dev* 1999; **89**: 155–159. [Medline] [CrossRef]
- Nakano K, Yamauchi J, Nakagawa K, Itoh H, Kitamura N. NESK, a member of the germinal center kinase family that activates the c-Jun N-terminal kinase pathway and is expressed during the late stages of embryogenesis. *J Biol Chem* 2000; **275**: 20533–20539. [Medline] [CrossRef]
- Dan I, Watanabe NM, Kusumi A. The Ste20 group kinases as regulators of MAP kinase cascades. *Trends Cell Biol* 2001; **11**: 220–230. [Medline] [CrossRef]
- Denda K, Nakao-Wakabayashi K, Okamoto N, Kitamura N, Ryu JY, Tagawa YI, Ichisaka T, Yamanaka S, Komada M. NrK, an X-linked protein kinase in the germinal center kinase family, is required for placental development and fetoplacental induction of labor. *J Biol Chem* 2011; **286**: 28802–28810. [Medline] [CrossRef]
- Lestari B, Naito S, Endo A, Nishihara H, Kato A, Watanabe E, Denda K, Komada M, Fukushima T. Placental mammals acquired functional sequences in NRK for regulating the CK2-PTEN-AKT pathway and placental cell proliferation. *Mol Biol Evol* 2022; **39**: 39. [Medline] [CrossRef]
- Liu G, Zhang C, Wang Y, Dai G, Liu SQ, Wang W, Pan YH, Ding J, Li H. New exon and accelerated evolution of placental gene NrK occurred in the ancestral lineage of placental mammals. *Placenta* 2021; **114**: 14–21. [Medline] [CrossRef]
- Denda K, Ida K, Tanno M, Nakao-Wakabayashi K, Komada M, Hayashi N. Proteomic analysis of NrK gene-disrupted placental tissue cells explains physiological significance of NRK. *BMC Res Notes* 2019; **12**: 785. [Medline] [CrossRef]
- Hu D, Cross JC. Development and function of trophoblast giant cells in the rodent placenta. *Int J Dev Biol* 2010; **54**: 341–354. [Medline] [CrossRef]
- Dilworth MR, Sibley CP. Review: Transport across the placenta of mice and women. *Placenta* 2013; **34**(Suppl): S34–S39. [Medline] [CrossRef]
- Biggers JD, Curnow RN, Finn CA, McLaren A. Regulation of the gestation period in mice. *J Reprod Fertil* 1963; **6**: 125–138. [Medline] [CrossRef]
- Murray SA, Morgan JL, Kane C, Sharma Y, Heffner CS, Lake J, Donahue LR. Mouse gestation length is genetically determined. *PLoS One* 2010; **5**: e12418. [Medline] [CrossRef]
- Morioka Y, Nam JM, Ohashi T. Nik-related kinase regulates trophoblast proliferation and placental development by modulating AKT phosphorylation. *PLoS One* 2017; **12**: e0171503. [Medline] [CrossRef]
- Simmons DG, Rawn S, Davies A, Hughes M, Cross JC. Spatial and temporal expression of the 23 murine Prolactin/Placental Lactogen-related genes is not associated with their position in the locus. *BMC Genomics* 2008; **9**: 352. [Medline] [CrossRef]
- Sugimoto Y, Yamasaki A, Segi E, Tsuboi K, Aze Y, Nishimura T, Oida H, Yoshida N, Tanaka T, Katsuyama M, Hasumoto K, Murata T, Hirata M, Ushikubi F, Negishi M, Ichikawa A, Narumiya S. Failure of parturition in mice lacking the prostaglandin F receptor. *Science* 1997; **277**: 681–683. [Medline] [CrossRef]
- Tsuboi K, Iwane A, Nakazawa S, Sugimoto Y, Ichikawa A. Role of prostaglandin H2 synthase 2 in murine parturition: study on ovariectomy-induced parturition in prostaglandin F receptor-deficient mice. *Biol Reprod* 2003; **69**: 195–201. [Medline] [CrossRef]
- Mahendroo MS, Cala KM, Russell DW. 5 alpha-reduced androgens play a key role in murine parturition. *Mol Endocrinol* 1996; **10**: 380–392. [Medline]
- Mahendroo MS, Porter A, Russell DW, Word RA. The parturition defect in steroid 5alpha-reductase type 1 knockout mice is due to impaired cervical ripening. *Mol Endocrinol* 1999; **13**: 981–992. [Medline]
- Piekorz RP, Gingras S, Hoffmeyer A, Ihle JN, Weinstein Y. Regulation of progesterone levels during pregnancy and parturition by signal transducer and activator of transcription 5 and 20alpha-hydroxysteroid dehydrogenase. *Mol Endocrinol* 2005; **19**: 431–440. [Medline] [CrossRef]
- Vannuccini S, Bocchi C, Severi FM, Challis JR, Petraglia F. Endocrinology of human parturition. *Ann Endocrinol (Paris)* 2016; **77**: 105–113. [Medline] [CrossRef]